Article No. jmbi.1999.3322 available online at http://www.idealibrary.com on IDEAL® J. Mol. Biol. (2000) 295, 117–125

JMB

Helix Tilt of the M2 Transmembrane Peptide from Influenza A Virus: An Intrinsic Property

F. A. Kovacs[1,2], Jeffrey K. Denny[1,3], Z. Song[1], J. R. Quine[1] and T. A. Cross[1,2,4]*

[1]*The National High Magnetic Field Laboratory*

[2]*Institute of Molecular Biophysics*

[3]*Department of Mathematics and*

[4]*Department of Chemistry Florida State University Tallahassee, FL, 32306-4005, USA*

**Corresponding author*

Solid-state NMR has been used to study the influence of lipid bilayer hydrophobic thickness on the tilt of a peptide (M2-TMP) representing the transmembrane portion of the M2 protein from influenza A. Using anisotropic ^{15}N chemical shifts as orientational constraints, single-site isotopically labeled M2-TMPs were studied in hydrated dioleoylphosphatidylcholine (DOPC) and dimyristoylphosphatidylcholine (DMPC) lipid bilayers oriented between thin glass plates. These chemical shifts provide orientational information for the molecular frame with respect to the magnetic field in the laboratory frame. When modeled as a uniform ideal α-helix, M2-TMP has a tilt of 37(±3)° in DMPC and 33(±3)° in DOPC with respect to the bilayer normal in these lipid environments. The difference in helix tilt between the two environments appears to be small. This lack of a substantial change in tilt further suggests that significant interactions occur between the helices, as in an oligomeric state, to prevent a change in tilt in thicker lipid bilayers.

Keywords: solid state NMR; membrane protein; ion channel; ^{15}N chemical shift; orientational constraints

Introduction

Unlike water-soluble proteins, the orientation of membrane proteins relative to their environment is critical. Consequently, the tilt of transmembrane α-helices relative to the bilayer may be an intrinsic property of the protein. However, when a protein has a single transmembrane α-helix, the tilt of the helix may simply reflect a match of the hydrophobic length of the peptide with the hydrophobic dimension of the bilayer. A greater length of peptide would result in a greater angle of the helix axis to the bilayer normal. If such a protein formed an oligomeric state, the tilt might or might not be affected by the hydrophobic thickness of the bilayer depending on whether or not the interactions between the monomers were sufficiently specific and strong to withstand a hydrophobic mismatch between the hydrophobic domain of the bilayer and peptide.

Influenza A is an enveloped virus with an RNA/protein core enclosed by a lipid bilayer. This lipid envelope contains a number of membrane proteins responsible for successful infection of a host cell. The virus invades the cell *via* endocytosis following recognition by cellular receptors leading to endosome formation. The M2 protein in the lipid envelope of the virus is activated by the low pH of the endosome and allows protons to pass into the core of the virion (Hay, 1992; Sugrue & Hay, 1991). Low pH in the viral core then causes the dissociation of the RNA/protein complex prior to fusion of the viral membrane with the endosomal membrane. The free RNA can then be read and copied for the production of new viral particles (Hay, 1992; Lamb & Krug, 1996).

The M2 protein has 97 amino acid residues with 24 extracellular, 19 transmembrane and 54 intracellular (Lamb *et al*., 1985). It forms a tetramer either as disulfide-linked dimers or as a completely disulfide-linked tetramer (Holsinger & Lamb, 1991; Panayotov & Schlesinger, 1992; Sugrue & Hay, 1991). The ion channel activity of the M2 protein has been well characterized (Pinto *et al*., 1992; Shimbo *et al*., 1996; Wang *et al*., 1993). The antiviral

Abbreviations used: DMPC, dimyristoylphosphatidylcholine; DOPC, dioleoylphosphatidylcholine; M2-TMP, M2 protein transmembrane peptide; SS NMR, solid-state nuclear magnet resonance.

E-mail address of the corresponding author: cross@magnet.fsu.edu

0022-2836/00/010117–9 $35.00/0

drugs amantadine (Duff *et al*., 1992; Wang *et al*., 1993) and BL-1743 (Tu *et al*., 1996) are known to reversibly block proton conductance. By using mixed oligomers of amantadine-sensitive and resistive mutant proteins in conductance studies, it has been demonstrated that the active oligomeric form of M2 protein is homotetrameric (Sakaguchi *et al*., 1997).

A peptide (M2-TMP) (NH_2-Ser_{22}-Ser_{23}-Asp_{24}-Pro_{25}-Leu_{26}-Val_{27}-Val_{28}-Ala_{29}-Ala_{30}-Ser_{31}-Ile_{32}-Ile_{33}-Gly_{34}-Ile_{35}-Leu_{36}-His_{37}-Leu_{38}-Ile_{39}-Leu_{40}-Trp_{41}-Ile_{42}-Leu_{43}-Asp_{44}-Arg_{45}-Leu_{46}- CO_2H) containing the predicted transmembrane portion of the M2 protein (Pro_{25}-Leu_{43}) has been observed to conduct protons (Duff & Ashley, 1992). Circular dichroism studies of the M2-TMP show the transmembrane region to be primarily (85-90 %) α-helical (Duff *et al*., 1992; Kovacs & Cross, 1997). Recently, sucrose density-centrifugation studies of M2-TMP in micelles have shown the peptide to associate as tetramers (Salom *et al*., 1999). These lines of evidence support a tetrameric α-helical bundle model for M2-TMP in hydrated lipid bilayers.

Solid-state NMR is rapidly developing as an approach for achieving membrane protein structures (Cross, 1994; Fu & Cross, 1999). While several different approaches for obtaining solid-state NMR-derived structural constraints have been developed, here, orientational constraints are gained through the observation of uniformly aligned lipid bilayer preparations of M2-TMP. Specifically, the peptide orientation is determined by measuring anisotropic ^{15}N chemical shifts and ^{15}N-^{1}H dipolar splittings of the M2-TMP incorporated into different hydrated lipid environments aligned between thin glass plates. The chemical shift has an orientational dependence with respect to the magnetic field, **B**. If the magnitude of the chemical shift shielding tensor elements and their orientation is known with respect to the molecular frame, i.e. the covalent bonds to the ^{15}N atom, then the orientation of this molecular site can be constrained with respect to the magnetic field axis. The ^{15}N-^{1}H dipolar splitting is dependent on the orientation of the unique dipolar interaction tensor element, which lies along the NH bond vector, with respect to **B**. This dipolar orientational constraint can be used to determine whether a change in orientation of the helix occurs. In a number of previous studies, solid-state NMR has been used sucessfully to study protein structure in membrane environments using such orientational constraints (Cross, 1994; Cross & Opella, 1994; Gröbner *et al*., 1998; Ketchem *et al*., 1993, 1996; Kim *et al*., 1998; Shon *et al*., 1991; Opella *et al*., 1999).

Using just five anisotropic ^{15}N chemical shift measurements, M2-TMP was previously modeled as a regular α-helix ($\phi = -65^\circ$, $\psi = -40^\circ$) tilted by $33(\pm3)^\circ$ from the bilayer normal (Kovacs & Cross, 1997). All of the initial data were collected on peptides oriented in dimyristoylphosphatidylcholine (DMPC). Here, additional data are presented for DMPC and efforts have been made to study the peptide orientation in the longer chain lipid dioleoylphosphatidylcholine (DOPC), to see how this tilt value is affected by the hydrophobic thickness of the bilayer.

Results

Circular dichroism spectra of M2-TMP in both DMPC and DOPC vesicles at an 8:1 lipid to peptide molar ratio and a peptide concentration of 40 μg/ml are shown in Figure 1. The spectra show that the peptide is predominantly α-helical (85-90 %) as characterized by minima at 208-210 nm and 220 nm as well as a maximum near 190-193 nm (Yang *et al*., 1986).

^{15}N chemical shift spectra of ^{15}N-labeled Val_{27} M2-TMP in various lipid preparations are shown in Figure 2. Initial samples of DOPC and peptide oriented between glass plates were made at the same molar ratio as DMPC; however, the spectra for all of these samples showed broad peaks with chemical shifts near the isotropic value. Such resonance frequencies can arise from a tensor orientation near the magic angle or from molecular motions that average the tensor to a near-isotropic value. Some of these DOPC samples showed both isotropic and non-isotropic chemical shifts indicating the coexistence of different peptide environments. Additionally, ^{31}P spectra for these samples also indicated the presence of an isotropic lipid phase. Subsequent DOPC samples made at a molar ratio of 30:1 (Figure 2(c)) showed no indication of an isotropic peak. ^{15}N chemical shift spectra were recorded for a number of peptides oriented in both hydrated DMPC and DOPC bilayers and the chemical shift values are listed in Table 1. Typically, linewidths of 15-20 ppm are observed.

The static principal values of the ^{15}N tensor for ^{15}N-labeled Val_{27} M2-TMP were characterized from a dry sample of the peptide (Figure 2(a)) by recording a ''powder pattern'' spectrum of a randomly dispersed powder sample. Through spectral simulation, the tensor elements were obtained: $\sigma_{11} = 31$, $\sigma_{22} = 55$ and $\sigma_{33} = 199(\pm2)$ ppm. The

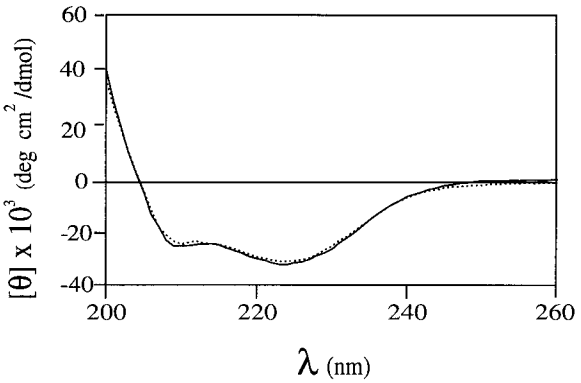

Figure 1. CD spectra for M2-TMP incorporated into DMPC (------) and DOPC (—) vesicles at a lipid to peptide molar ratio of 8 to 1.

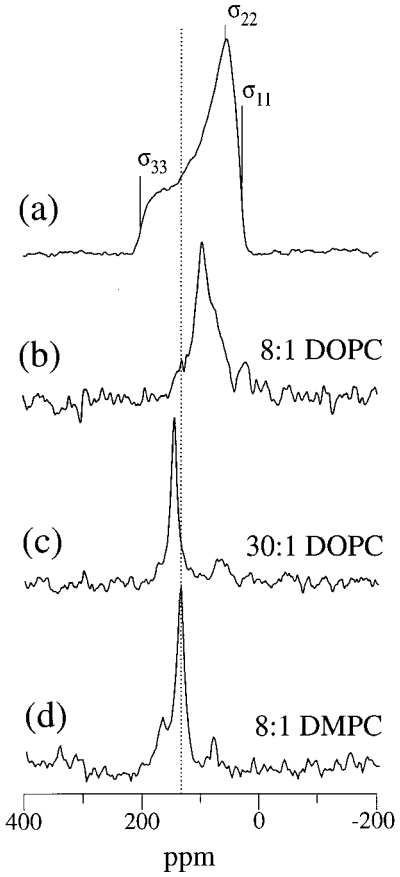

Figure 2. ^{15}N chemical shift spectra of ^{15}N-labeled Val_{27} M2-TMP recorded at 40.6 MHz and 25 °C in (a) dry powder, which provides a measurement of the principal elements of the chemical shift shielding tensor ($\sigma_{11} = 31$, $\sigma_{22} = 55$, $\sigma_{33} = 199 \pm 2$ ppm), (b) oriented in DOPC at a lipid to peptide molar ratio of 8 to 1, (c) oriented in DOPC at 30:1 and (d) oriented in DMPC at 8:1. The resonance at 85 ppm is from the $\sigma_\perp$ component of the residual powder pattern. The assignment of the resonance at 175 ppm is less certain, but may reflect partial drying of the sample, its appearance is intermitent. Samples (b)-(d) were approximately 50 % (w/w).

isotropic chemical shift is the average of these principal values, $\sigma_{iso} = 95$ ppm, close to the observed value in Figure 2(b) of 97(±5) ppm. Here, the tensors are characterized for the specific sites of interest. Since the powders were dried from trifluoroethanol where the peptide is observed to be α-helical, it is likely that the peptides are in the conformation of interest. To achieve static and librationally averaged tensor element magnitudes in lipid bilayer environments is very challenging (Lazo *et al.*, 1993). Because of the uniform secondary structure, it is assumed that the librational averaging is similar throughout and similar to that in a dry powder; a result that is consistent with previous findings (Mai *et al.*, 1993). Furthermore, it is assumed that the dynamics in DOPC and DMPC are the same. The tensor element magnitudes are included in Table 1.

In the previous study, the helix axis was visually alligned and orthogonal axes were arbitrarily defined (Kovacs & Cross, 1997). Here, the helix axis frame (HAF) is mathematically defined with the frame described by the vectors $\mathbf{h}_1$, $\mathbf{h}_2$ and $\mathbf{h}_3$ (Figure 3). In this frame, $\mathbf{h}_3$ is a unit vector in the direction of the helix axis (positive direction from N to C terminus), $\mathbf{h}_1$ is the unit vector perpendicular to $\mathbf{h}_3$ pointing from the helix axis to the C^α of Leu_{26}, and $\mathbf{h}_2 = \mathbf{h}_3 \times \mathbf{h}_1$. This frame is denoted by HAF(k), where k is the residue number. If a vector $\mathbf{v}$ can be written as:

$$\mathbf{v} = x\mathbf{h}_1 + y\mathbf{h}_2 + z\mathbf{h}_3$$

then (x,y,z) will be referred to as the coordinates of $\mathbf{v}$ in HAF. This frame of reference differs from that used previously (Kovacs & Cross, 1997) by a rotation about $\mathbf{h}_3$ of −240 ° and the opposite handedness of the direction, so that $\rho = -14°$ rather than 254 °.

The position of the helix axis relative to **B** can be determined by the polar coordinates, ρ and τ, of **B** in HAF(26). More specifically, the coordinates of **B** in HAF(26) are (sin τ cos ρ, sin τ sin ρ, cos τ).

For a regular α-helix, the coordinates of **B** in HAF(k) are given by the vector:

$$B(\rho, \tau, k) = (\sin\tau\cos(\rho - (k-26)100°), \times \sin\tau\sin(\rho - (k-26)100°), \cos\tau)$$

since the HAF rotates 100 ° around the helix axis direction for each residue in this ideal helix. For all of the peptide samples used in this study, the bilayer normal is oriented parallel with **B**. The tilt angle, τ, is easily visualized as the angle between the helix axis, $\mathbf{h}_3$, and the bilayer normal, equivalent to **B**. The helix axis rotation angle, ρ, is defined as the angle between $\mathbf{h}_1$ and the projection of **B** into the h_1h_2 plane (Figure 3).

Consider the principal axis frame (PAF) for the ^{15}N chemical shift tensor at residue k, PAF(k), in which the chemical shift tensor has the diagonal form:

$$\sigma = \begin{bmatrix} \sigma_{11,k} & 0 & 0 \\ 0 & \sigma_{22,k} & 0 \\ 0 & 0 & \sigma_{33,k} \end{bmatrix}$$

where $\sigma_{11,k}$, $\sigma_{22,k}$ and $\sigma_{33,k}$ are the principal values of the chemical shift tensor for the kth residue. The orientation of the tensor or PAF with respect to the molecular frame is specified by the Euler angles $\alpha_D = 0°$ and $\beta_D = 105°$ from model systems (Mai *et al.*, 1993; Teng & Cross, 1989). The matrix that transforms the coordinates from PAF(k) to HAF($k-1$) can be computed as:

$$R = \begin{bmatrix} -0.83 & 0.56 & -0.04 \\ 0.55 & 0.08 & -0.22 \\ -0.09 & -0.21 & -0.97 \end{bmatrix}$$

Table 1. ^{15}N anisotropic chemical shift data (in ppm)

Site	DMPC[a]	DOPC[b]	σ_{11}	σ_{22}	σ_{33}
Val_{27}	136 ± 5	147 ± 5	31 ± 2	55 ± 2	199 ± 2
Val_{28}	107	120	29	53	202
Ile_{32}	124		35	59	208
Ile_{33}	172	170	31	54	202
Ile_{35}	116		32	56	210
Ile_{39}	130	129	30	54	195
Leu_{40}	151	160	32	55	203
Trp_{41}	177	184	32	56	205
Ile_{42}	129	137	30	54	198
Leu_{43}	127	137	29	56	200

[a] Molar ratio of peptide to lipid, 1:8.
[b] Molar ratio of peptide to lipid, 1:30.

for an ideal α-helix. Since the helix is regular, this matrix is independent of k. The chemical shift at residue k is then given by the function:

$$f(\sigma_{11,k}, \sigma_{22,k}, \sigma_{33,k}, \rho, \tau, k) = B(\rho, \tau, k-1)R\sigma R'B(\rho, \tau, k-1)'$$

where the prime denotes the matrix transpose.

Using the two sets of data (DMPC and DOPC) in Table 1, best fit orientations of a model ideal helix relative to **B** and the bilayer normal were determined for these two environments. Briefly, **B** is rotated over all ρ and τ space and chemical shifts are calculated for each experimentally characterized site. The root-mean-squared deviation (RMSD) between the observed and calculated chemical shifts is calculated over all possible orientations of **B** (Figure 4). A minimum RMSD is defined as the best fit orientation ($\tau = 37°$, $\rho = -10°$ for DMPC; $\tau = 33°$, $\rho = -4°$ for DOPC). The minimum RMSD values are quite

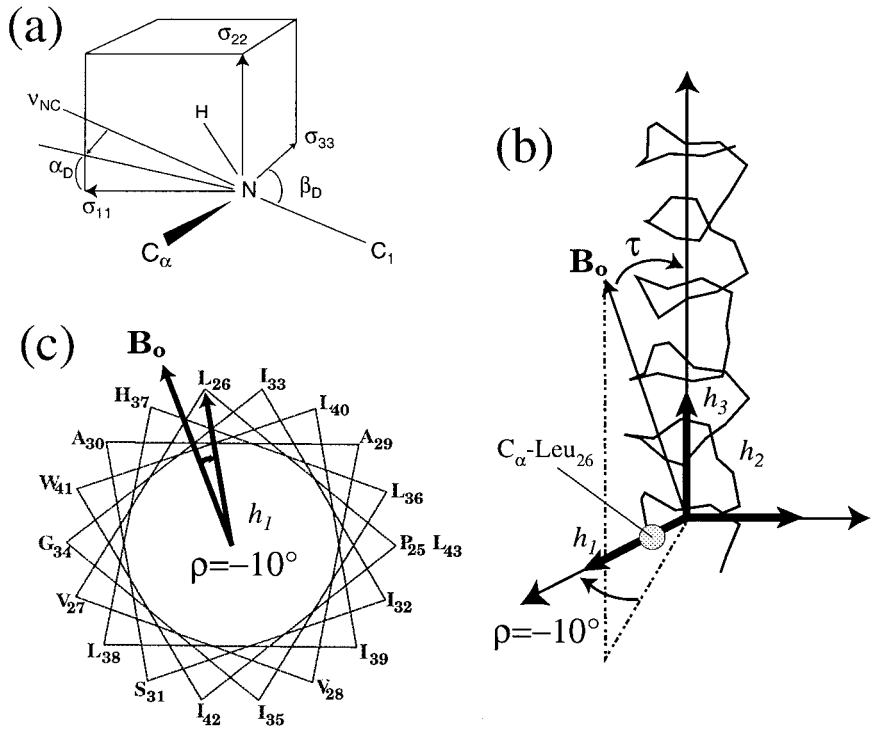

Figure 3. (a) The orientation of the ^{15}N chemical shift tensor relative to the molecular frame is given by α_D and β_D. (b) M2-TMP is modeled as an ideal α-helix in the helix axis frame, $\mathbf{h}_1$, $\mathbf{h}_2$ and $\mathbf{h}_3$, where $\mathbf{h}_3$ is equivalent to the helix axis in the direction from N to C terminus, $\mathbf{h}_1$ is defined as going from the helix axis through the C^{α} of Leu_{26} and $\mathbf{h}_2$ as the cross-product of $\mathbf{h}_3$ and $\mathbf{h}_1$. The polar coordinates for the magnetic field axis, **B**, is given by ρ and τ. The origin (0°) for τ is $\mathbf{h}_3$ parallel with the bilayer normal. (c) The origin (0°) for ρ is $\mathbf{h}_2$ parallel with the $\mathbf{B}_{\perp}$ component as viewed down the $\mathbf{h}_3$ axis.

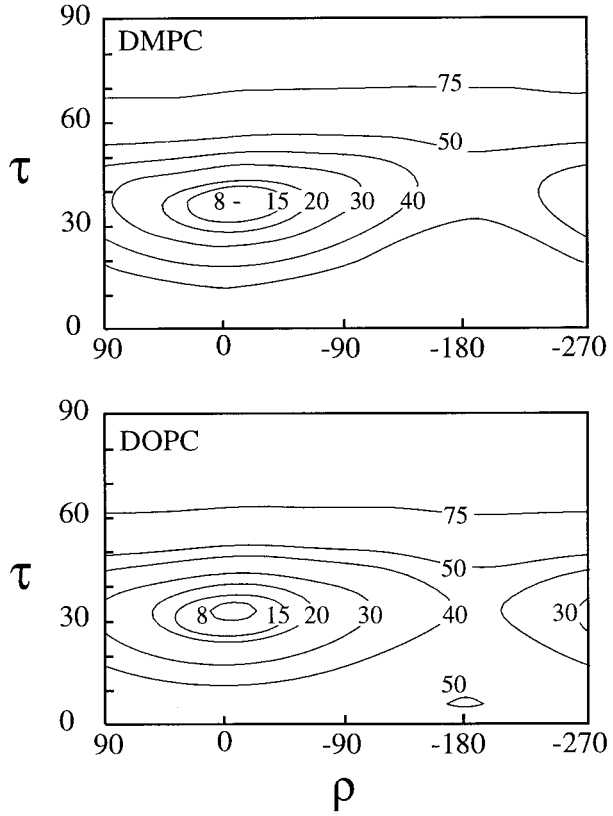

Figure 4. The RMSD of the experimental and calculated chemical shifts was determined for all orientations of **B** with ρ ranging from 0° to 360° and τ from 0° to 90°. The results are plotted here using the data from Table 1 for both (a) DMPC and (b)DOPC. The minima are found to lie at (a) $\rho = -10°$ and $\tau = 37°$ and (b) $\rho = -4°$ and $\tau = 33°$.

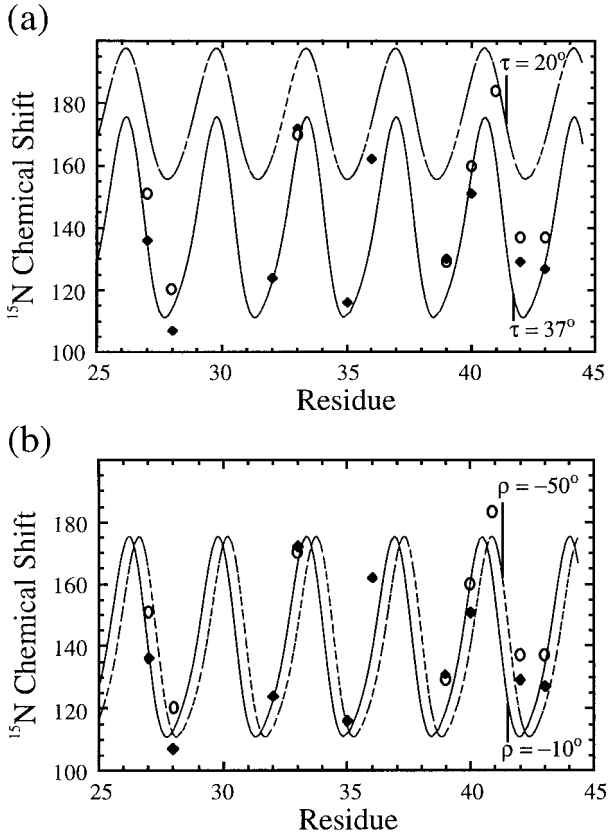

Figure 5. Functions are shown illustrating the influence of τ and ρ on the pattern of chemical shifts to be anticipated from an ideal helix. (a) The chemical shift function for **B** oriented at $\rho = -10°$ with $\tau = 37°$ (—) and $\tau = 20°$ (-----). (b) The chemical shift function for **B** oriented at $\tau = 37°$ with $\rho = -10°$ (—) and $\rho = -50°$ (-----). These curves were calculated with $\alpha_D = 0°$, $\beta_D = 105°$, $\sigma_{11} = 32$ ppm, $\sigma_{22} = 55$ ppm, $\sigma_{33} = 200$ ppm, where the σ_{ii} values represent the average values based on the data in Table 1. The chemical shift data for DMPC (diamond) and DOPC (O) are shown on both plots.

high, 7.9 ppm for DMPC and 5.1 ppm for DOPC, reflecting the imperfect fit of an ideal helical model to the experimental sample and the relatively large experimental error bar. The associated error with the characterization of τ is estimated to be ± 3° and for ρ it is ± 20°.

The sensitivity of the data to ρ and τ is illustrated in Figure 5, where a sinusoidal function is displayed as a function of position along the helical trace of the C^{α} backbone positions. In Figure 5(a), two values of τ (37° and 20°) are shown each with $\rho = -3°$. The predicted orientation of the helix in DOPC is given by $\tau = 20°$, assuming that the helix tilt simply reflects the hydrophobic thickness of the bilayer and the hydrophobic length of the polypeptide. Since DOPC is approximately 4 Å thicker than DMPC (Weiner & White, 1992), the orientation would be predicted to change by 17°. Clearly, while there has been a modest change in some of the chemical shifts there has been no substantial change in τ.

A change in τ represents an offset in the sinusoidal curves, while a change in ρ represents a change in phase (Figure 5). Clearly, as indicated in Figure 4, the data do not so precisely characterize ρ as τ. Moreover, both Figure 5(a) and (b) show that the fit to the data with this regular sinusoidal curve generated from an ideal helix is far from perfect, but it is clear that the tilt of the helix is very sensitive to the chemical shifts and that an average tilt can be determined with considerable precision.

Figure 6 provides an example of DMPC and DOPC data along with spectral simulation for two sites (^{15}N-labeled Leu_{40} and ^{15}N-labeled Leu_{43}), assuming an ideal helix tilted at 37° and 20°, while the ρ value was constant at −10°. The change in chemical shift is relatively small compared to the resonance linewidth and much smaller than the predicted change for a 17° change in helix tilt. The two-dimensional PISEMA spectra (Wu *et al.*, 1994), which shows both the ^{15}N chemical shift and ^{15}N-^{1}H dipolar splitting, were obtained for ^{15}N-labeled Val_{27} M2-TMP oriented in DMPC

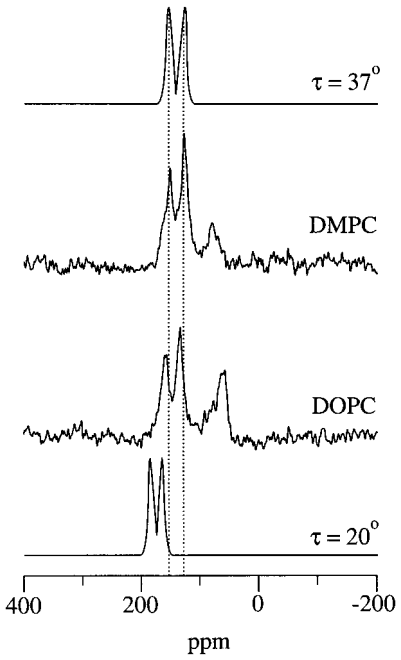

Figure 6. The ^{15}N chemical shift spectra were recorded for ^{15}N-labeled $Leu_{40,43}$ M2-TMP in hydrated (50 %, w/w) DMPC and DOPC bilayers aligned with the bilayer normal parallel with **B**. Also, shown here are the predicted spectra for an orientation of **B** with the polar coordinates of $\rho = -10°$ and $\tau = 37°$ (top) and $\rho = -10°$ and $\tau = 20°$ (bottom) with respect to the helix axis frame at Leu_{26}.

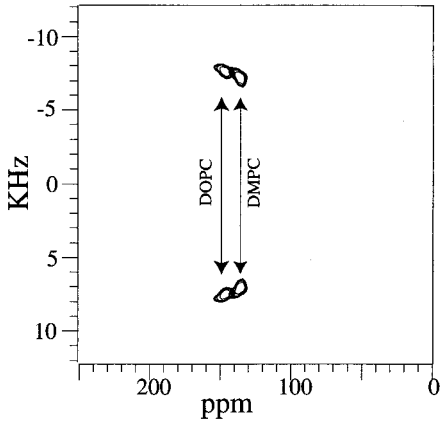

Figure 7. Overlay of 2D PISEMA spectra of single site labeled, oriented ^{15}N-[Val_{27}]-M2TMP in hydrated DMPC and DOPC lipid bilayers.

and DOPC (Figure 7). It is clear that both the summed interactions, as well as individual data sets, do not support a significant change in helix tilt upon going to DOPC.

Discussion

The concept of lipid bilayers as well-defined hydrophilic and hydrophobic slabs is giving way to that of a substantial interface region characterized by a polarity gradient (Weiner & White, 1992). However, it is still useful to discuss the definition of the hydrophobic thickness of a bilayer (Scherer, 1989), particularly when examining its affect on the structure or function of a protein. A number of researchers have explored hydrated bilayer structure using neutron and X-ray lamellar diffraction data (Lewis & Engelman, 1983; Weiner & White, 1992). From these types of data, the mean carbonyl position is the best characterized position and can be used to define the limit of the hydrophobic region. For the lipids used in this study, the hydrophobic thickness for fully hydrated bilayers has been taken from the literature to be 23 Å for DMPC (Lewis & Engelman, 1983) and 27 Å for DOPC (Weiner & White, 1992).

The α-helical model of M2-TMP as a peptide tilted in the lipid bilayer environment is supported by the additional data. The CD data for this peptide in DMPC and DOPC vesicles confirms previous CD results (Duff *et al.*, 1992; Kovacs & Cross, 1997) demonstrating that the peptide is predominately α-helical in the lipid membrane environments. It is assumed here that the hydrophobic environment of the lipid vesicle closely models that of hydrated, stacked lipid bilayers present in our oriented samples. Since the CD results indicate a high percentage of α-helix, our present model is α-helical for residues 26-43 (72 % of the polypeptide residues). While our data suggest the posibility of some non-uniformity for this α-helix, it is not possible with the limited data available to define the helical distortions uniquely. The NMR spectra of the oriented samples continue to support the presence of a single primary conformation and orientation for this peptide. This is shown in Figures 2, 6 and 7 by the presence of single peaks for each labeled site. Therefore, if the peptide is part of an oligomer, it must be a symmetric or at least pseudo-symmetric bundle.

A recent study using attenuated total reflectance Fourier transform infrared (ATR-FTIR) spectroscopy was performed on M2-TMP reconstituted into DMPC vesicles (Kukol *et al.*, 1999). Two orientational constraints were obtained from $^{13}C_1$-labeled Ala_{29} and $^{13}C_1$-labeled Ala_{30} M2-TMPs with an order parameter experimentally determined from the dichroic ratio. Using a molecular dynamics procedure, an orientational refinement was performed on the M2-TMP bundle. This analysis produced a tilt angle for the helix of 31.6(±6.2)°, which is similar to the tilt of the models described here.

The data presented here suggest that there is an association of the peptides that prevents a significant change in the tilt of the peptides upon modifying the bilayer hydrophobic thickness. Furthermore, this association is specific enough that the helical bundle is modified only slightly when strained in DOPC. The lipid-induced strain is suggested by the formation of a non-bilayer

phase in samples with an 8:1 molar ratio of DOPC to peptide (Figure 2). Although this ratio did not appear to be a problem with DMPC, it became apparent immediately that an isotropic lipid phase was present in the DOPC samples of the same molar ratio, as evidenced by isotropic chemical shifts in both ^{15}N and ^{31}P spectra. This type of behavior has been observed and identified as a cubic phase for hydrophobic peptides in hydrated lipid samples with known hydrophobic mismatch (Killian *et al*., 1996; Killian, 1998; de Planque *et al*., 1998). Killian and co-workers showed that the presence of non-bilayer lipid phases could be correlated to the extent of mismatch between the length of the hydrophobic region of the incorporated peptide and the width of the hydrocarbon region of the lipid bilayer. For the work presented here, this suggested that the presence of the isotropic phase in our samples was due to a hydrophobic mismatch. The phase diagram for these cubic phases is such that they disappear as the concentration of peptide is lowered (Killian *et al*., 1996; Morein *et al*., 1997). Therefore, additional DOPC samples were prepared at a lipid to peptide molar ratio of 30:1. For these samples, the ^{15}N chemical shift spectra showed no detectable presence of an isotropic chemical shift. While the data do not give direct support for a four-helix model in our preparations, it does suggest a specific association of the peptides that substantially prevents rearrangement of the helices to accommodate a thicker hydrophobic region through a smaller tilt angle in DOPC. In other words, there is no reason to believe that a monomer would not decrease it's tilt in the bilayer as the hydrophobic thickness is increased (de Planque *et al*., 1998) by 4 Å in going from DMPC to DOPC bilayers. Since this result was not observed, the results suggest that the polypeptide is in an oligomeric state with a constrained tilt angle with respect to the bilayer normal.

As noted previously (Kovacs & Cross, 1997), the hydrophilic residues in the transmembrane segment (Ser_{31}, His_{37} and Trp_{41}) can be arranged on the inside of a bundle with these values of ρ and τ if a left-handed packing arrangement of the monomers is used. This four-helix bundle is not as stable as might be expected for a typical water-soluble protein stabilized by hydrogen bonds and numerous electrostatic interactions, as well as van der Waals interactions. In this bilayer-bound bundle, there will be few if any intermonomer hydrogen bonds or electrostatic interactions; instead, the interactions will be dominated by van der Waals interactions. Even hydrophobic interactions will be minimized, since the monomer environment is itself hydrophobic. Consequently, while the interaction between monomers appears to have some preferred surface, it is possible to distort the structures slightly through changing the bilayer environment. This is consistent with the recent cysteine mutagenesis and cross-linking studies by Lamb, Pinto and co-workers (Bauer *et al*., 1999) in which significant rotational flexibility for the monomers was noted. Here, NMR has described time-averaged values for the helix tilt and rotation angle. These do not change by many degrees upon making the hydrophobic dimension 4 Å thicker. Furthermore, if large dynamic excursions occurred even infrequently, it could be anticipated that the hydrophobic mismatch could have been tolerated without a change in the lipid phase. Therefore, these results suggest that only modest flexibility occurs at the helix-helix interface in M2-TMP.

Materials and Methods

The isotopically labeled amino acids, [^{15}N]Leu, [^{15}N]Ile, and [^{15}N]Val were purchased from Cambridge Isotope Laboratories (Cambridge, MA) and used to prepare the Fmoc derivatives (Fields *et al*., 1989; Fields *et al*., 1988). All of the peptides were made using solid phase peptide synthesis on an Applied Biosystems 430A peptide synthesizer (Foster City, CA) and cleaved from the resin as described (Kovacs & Cross, 1997). These peptides were characterized using amino acid sequencing of the five N-terminal amino acid residues and gradient correlation spectroscopy (GCOSY) in organic solution by NMR as described (Kovacs & Cross, 1997).

Secondary structure of M2-TMP was characterized using CD of the peptide incorporated into dimyristoylphosphatidylcholine (DMPC) (Sigma, St. Louis, MO) and dioleoylphosphatidylcholine-9 cis (DOPC) (Avanti Polar Lipids, Alabaster, AL) vesicles. Samples were prepared by cosolubilizing the lipid and peptide at an 8 to 1 molar ratio, in trifluoroethanol (TFE), which was subsequently dried under reduced pressure. The vesicles were formed by adding water to the sample (peptide concentration ~40 μg/ml) and then sonicating for 15 minutes in a water-bath. The CD spectra were recorded on an AVIV model 62A DS (Lakewood, NJ) CD spectrometer.

Oriented samples of the peptide in hydrated lipid bilayers were prepared by first cosolubilizing M2-TMP (~25 mg) and either DMPC(~50 mg) or DOPC(~200 mg) in 700 μl of TFE. This solvent was found to better solubilize the peptide than methanol, which was used previously. The solution was then spread onto 60 glass plates (75 μm × 10.5 mm × 10.5 mm) and allowed to air-dry for 12 hours. The plates were vacuum-dried for at least 24 hours. Square glass tubing (11 mm × 11 mm i.d.) was cut to a height of 8 mm and sealed at one end with epoxy and a microscope cover-glass (13 mm × 13 mm). The dried plates were placed into the square glass sample holder and HPLC-grade water was added to each slide as it was stacked to achieve a hydration of 50% (w/w). This sample was then sealed with a second cover-glass and incubated at 45 °C for one to two weeks.

^{31}P NMR was performed on a narrow-bore IBM/Bruker 200SY spectrometer with a home-built solids package. A double-resonance $^{31}P/^{1}H$ probe was used for proton decoupling. All of the ^{31}P experiments were performed at a resonant frequency of 80.99 MHz, with a recycle delay of four seconds and a 90° pulse width of 11 μs. The 1D ^{15}N chemical shift spectra were obtained on a home-built 400 MHz spectrometer, using a Chemagnetics data acquisition system and a wide-bore Oxford Instruments 400/89 magnet. A home-built double-frequency probe was used with a proton decoupling field strength of 70 kHz. Spectra were obtained with cross-polarization at a resonance frequency of 40.6

MHz with a contact time of 1 ms, recycle delay of four seconds, and a 90° pulse width of 6.0 μs. A Hahn echo was used with 40 μs intervals to minimize probe ringing influences.

For the PISEMA experiment (Wu *et al*., 1994), a cross-polarization (CP) period of ~1 ms was used. The rf strengths were typically 31.4 kHz in CP match, and 38.5 kHz in LG match, corresponding to each LG duration $t_m = 26$ μs. Prior to each ± LG cycle, a delay of 1 μs was given to compensate for the frequency synthesizer (PTS type) switch time. This was found to be critical for achieving the correct scaling factor (0.816, theoretically) in the dipolar dimension. The t_1 was incremented in 0-24 LG cycles, and the refocused S-signal was acquired with ~2000 transients for each t_1. The spectra were processed using 512 and 256 points in the t_2 and t_1 dimensions, respectively. Exponential line broadening of 100 Hz was applied in t_2. In the t_1 dimension, the imaginary part of the data was set to zero prior to Fourier transformation to obtain spectral symmetry.

Acknowledgments

The authors are indebted to the staff of the NHMFL and FSU NMR facilities, to J. Vaughn and A. Blue as well the staff of the Bioanalytical Synthesis and Services Laboratory, and to H. Henricks and U. Goli for their expertise and maintenance of the instrumentation essential for this effort. This work was supported by the National Science Foundation, DMB 9603935 (T.A.C.) and DBI 9602233 (J.K.D.). The work was performed largely at the National High Magnetic Field Laboratory supported by NSF Cooperative Agreement (DMR-9527035) and the State of Florida.

References

Bauer, C. M., Pinto, L. H., Cross, T. A. & Lamb, R. A. (1999). The influenza virus M2 ion channel protein probing the structure of the transmembrane domain in intact cells by using engineered disulfide cross-linking. *Virology,* **254**, 196-209.

Cross, T. A. (1994). Structural biology of peptides and proteins in synthetic membrane environments by solid-state NMR Spectroscopy. *Annu. Rep. NMR Spectrosc.* **29**, 124-167.

Cross, T. A. & Opella, S. J. (1994). Solid-state NMR structural studies of peptides and proteins in membranes. *Curr. Opin. Struct. Biol.* **4**, 574-581.

de Planque, M. R. R., Greathouse, D. V., Koeppe, R. E., Schafer, H., Marsh, D. & Killian, J. A. (1998). Influence of lipid/peptide hydrophobic mismatch on the thickness of diacylphosphatidylcholine bilayers. A ^{2}H NMR and ESR study using designed transmembrane α-helical peptides and gramicidin A. *Biochemistry,* **37**, 9333-9345.

Duff, K. C. & Ashley, R. H. (1992). The transmembrane domain of influenza A M2 protein forms amantadine-sensitive proton channels in planar lipid bilayers. *Virology,* **190**, 485-489.

Duff, K. C., Kelly, S. M., Price, N. C. & Bradshaw, J. P. (1992). The secondary structure of influenza A M2 transmembrane domain. A circular dichroism study. *FEBS Letters,* **311**, 256-258.

Fields, C. G., Fields, G. B., Noble, R. L. & Cross, T. A. (1989). Solid phase peptide synthesis of ^{15}N-gramicidins A, B, and C and high performance liquid chromatographic purification. *Int. J. Pept. Protein Res.* **33**, 298-304.

Fields, G. B., Fields, C. G., Petefish, J., Wart, H. E. V. & Cross, T. A. (1988). Solid phase peptide synthesis and solid state NMR spectroscopy of [Ala_3-^{15}N][Val_1] gramicidin A. *Proc. Natl Acad. Sci. USA,* **85**, 1384-1388.

Fu, R. & Cross, T. A. (1999). Solid-state NMR magnetic resonance investigation of protein and polypeptide structure. *Annu. Rev. Biophys. Biomol. Struct.* **28**, 235-268.

Gröbner, G., Choi, G., Burnett, I. J., Glaubitz, C., Verdegem, P. J. E. & Watts, A. (1998). Photoreceptor *Rhodopsin*: structural and conformational study of its chromophore 11-cis retinal in oriented membranes by deuterium solid-state NMR. *FEBS Letters,* **422**, 201-204.

Hay, A. J. (1992). The action of adamantamines against influenza A virus: inhibition of the M2 ion channel protein. *Semin. Virol.* **3**, 21-30.

Holsinger, L. J. & Lamb, R. A. (1991). Influenza virus M2 integral membrane protein is a homotetramer stabilized by formation of disulfide bonds. *Virology,* **183**, 32-43.

Ketchem, R. R., Hu, W. & Cross, T. A. (1993). High-resolution conformation of gramicidin A in a lipid bilayer by solid state NMR. *Science,* **261**, 1457-1460.

Ketchem, R. R., Lee, K. C., Huo, S. & Cross, T. A. (1996). Macromolecular structural elucidation with solid-state NMR-derived orientational constraints. *J. Biomol. NMR,* **8**, 1-14.

Killian, J. A. (1998). Hydrophobic mismatch between proteins and lipids in membranes. *Biochim. Biophys. Acta,* **1376**, 401-416.

Killian, J. A., Salemink, I., de Planque, M. R. R., Lindblom, G., Koeppe, R. E., II & Greathouse, D. V. (1996). Induction of nonbilayer structures in diacylphosphatidylcholine model membranes by transmembrane α-helical peptides: importance of hydrophobic mismatch and proposed role of tryptophans. *Biochemistry,* **35**, 1037-1045.

Kim, Y., Valentine, K., Opella, S. J., Schendel, S. L. & Cramer, W. A. (1998). Solid-state NMR studies of the membrane-bound closed state of the colicin E1 channel domain in lipid bilayers. *Protein Sci.* **7**, 342-348.

Kovacs, F. A. & Cross, T. A. (1997). Transmembrane four-helix bundle of influenza A M2 protein channel: structural implications from helix tilt and organization. *Biophys. J.* **73**, 2511-2517.

Kukol, A., Adams, P., Rice, L. M., Brünger, A. T. & Arkin, I. T. (1999). Experimentally based orientational refinement of membrane protein models: a structure for the influenza A M2 H^+ channel. *J. Mol. Biol.* **286**, 951-962.

Lamb, R. A. & Krug, R. M. (1996). Orthomyxoviridae: the viruses and their replication. In *Fields Virology* (Fields, B. N., Knipe, D. M. & Howley, P. M., *et al*., eds), vol. 1353, Lippincot-Raven Publishers, Philadelphia.

Lamb, R. A., Zebedee, S. L. & Richardson, C. D. (1985). Influenza virus M2 protein is an integral membrane protein expressed on the infected-cell surface. *Cell,* **40**, 627-633.

Lazo, N. D., Hu, W., Lee, K.-C. & Cross, T. A. (1993). Rapidly-frozen polypeptide samples for characterization of high definition dynamics by solid-state

NMR spectroscopy. *Biochem. Biophys. Res. Commun.* **197**, 904-909.

Lewis, B. A. & Engelman, D. M. (1983). Lipid bilayer thickness varies linearly with acyl chain length in fluid phosphatidylcholine vesicles. *J. Mol. Biol.* **166**, 211-217.

Mai, W., Hu, W., Wang, C. & Cross, T. A. (1993). Orientational constraints as three-dimensional structural constraints from chemical shift anisotropy: the polypeptide backbone of gramicidin A in a lipid bilayer. *Protein Sci.* **2**, 532-542.

Morein, S., Strandberg, E., Killian, A., Persson, S., Arvidson, G., Koeppe, R. E., II & Lindblom, G. (1997). Influence of membrane-spanning α-helical peptides on the phase behavior of the dioleoylphosphatidylcholine/water system. *Biophys. J.* **73**, 3078-3088.

Opella, S. J., Marassi, F. M., Gesell, J. J., Valente, A. P., Kim, Y., Oblatt-Montal, M. & Montal, M. (1999). Structures of the M2 channel-lining segments from nicotinic acetylcholine and NMDA receptors by NMR spectroscopy. *Nature*, **6**, 374-379.

Panayotov, P. P. & Schlesinger, R. W. (1992). Oligomeric organization and strain-specific proteolytic modification of the virion M_2 protein of influenza A H1N1 viruses. *Virology*, **186**, 352-355.

Pinto, L. H., Holsinger, L. J. & Lamb, R. A. (1992). Influenza virus M2 protein has ion channel activity. *Cell*, **69**, 517-528.

Sakaguchi, T., Tu, Q., Pinto, L. H. & Lamb, R. A. (1997). The active oligomeric state of the minimalistic influenza virus M_2 ion channel is a tetramer. *Proc. Natl Acad. Sci. USA*, **94**, 5000-5005.

Salom, D., Lear, J. D. & DeGrado, W. F. (1999). Aggregation of influenza A M2 transmembrane segment in micelles. *Biophys. J.* **76**, A123.

Scherer, J. R. (1989). On the position of the hydrophobic/hydrophilic boundary. *Biophys. J.* **55**, 957-964.

Shimbo, K., Brassard, D. L., Lamb, R. A. & Pinto, L. H. (1996). Ion selectivity and activation of the M_2 ion channel of influenza virus. *Biophys. J.* **70**, 1335-1346.

Shon, K.-J., Kim, Y., Colnago, L. A. & Opella, S. J. (1991). NMR studies of the structure and dynamics of membrane-bound bacteriophage Pf1 coat protein. *Science*, **252**, 1303-1308.

Sugrue, R. J. & Hay, A. J. (1991). Structural characteristics of the M2 protein of influenza A viruses: evidence that it forms a tetrameric channel. *Virology*, **180**, 617-624.

Teng, Q. & Cross, T. A. (1989). The in situ determination of the ^{15}N chemical-shift tensor orientation in a polypeptide. *J. Magn. Reson.* **85**, 439-447.

Tu, W., Pinto, L. H., Luo, G., Shaughnessy, M. A., Mullaney, D., Kurtz, S., Krystal, M. & Lamb, R. A. (1996). Characterization of inhibition of M2 ion channel activity by BL-1743, an inhibitor of influenza A virus. *J. Virol.* **70**, 4246-4252.

Wang, C., Takeuchi, K., Pinto, L. H. & Lamb, R. A. (1993). Ion channel activity of influenza A virus M2 protein: characterization of the amantadine block. *J. Virol.* **67**, 5585-5594.

Weiner, M. C. & White, S. H. (1992). Structure of a fluid dioleoylphosphatidylcholine bilayer determined by joint refinement of x-ray and neutron diffraction data. III. Complete structure. *Biophys. J.* **61**, 434-447.

Wu, C. H., Ramamoorthy, A. & Opella, S. J. (1994). High resolution neteronuclear dipolar solid-state NMR spectroscopy. *J. Magn. Reson. ser. A*, **109**, 270-272.

Yang, J. T., Wu, C. S. & Martinez, H. M. (1986). Calculation of protein conformation from circular dichroism. *Methods Enzymol.* **130**, 208-269.

Edited by P. E. Wright

(Received 23 July 1999; received in revised form 19 October 1999; accepted 22 October 1999)